Multiflash Experiments Reveal a New Kinetic Phase of Photosystem II Manganese Cluster Assembly in *Synechocystis* sp. PCC6803 in Vivo†

Hong Jin Hwang and Robert L. Burnap*

Department of Microbiology and Molecular Genetics, Oklahoma State University, Stillwater, Oklahoma 74078

Received January 12, 2005; Revised Manuscript Received May 4, 2005

ABSTRACT: The assembly of Mn^{2+} ions into the H_2O oxidation complex (WOC) of the photosystem II (PSII) reaction center is a light-driven process, termed photoactivation. According to the "two-quantum" model, photoactivation involves two light-driven charge separations coupled to the photooxidation of Mn^{2+} in order to form the first stable intermediate in a process that culminates in the oxidative assembly of four Mn^{2+} ions and one Ca^{2+} ion to form the active, higher valence (Mn_4-Ca) center of the WOC. To better define the kinetics of the dark rearrangement and to gain some understanding of the basis for the very low quantum yield of the overall process, photoactivation experiments, involving different flash patterns, were conducted with *Synechocystis* sp. PCC6803. It was found that even the so-called first stable intermediate is readily lost during protracted (1−10 s) dark periods during photoactivation of *Synechocystis* cells. Low concentrations of the electron acceptor, DCBQ, improved the stability of the dark intermediates. The unstable photoactivation intermediates formed early in the photoactivation process were not, however, stabilized by the addition of Ca^{2+}, although the overall yield of photoactivation is enhanced by the additional Ca^{2+}. Measurements of the kinetics of fluorescence yield verify that Q_A^- to Q_B electron transfer rates change during the course of photoactivation as the high potential form of Q_A^- is converted to the low potential form and show that DCBQ acts as an efficient electron acceptor from Q_A^- even while in its high potential form. In addition the ∼150 ms phase corresponding to the originally described dark rearrangement of photoactivation, repetitive, double flash experiments, with a 10 s intervening dark period, reveals a faster, 15 ms phase that is accentuated by DCBQ.

The assembly of manganese ions into the water oxidation complex (WOC[1]) of the photosystem II (PSII) reaction center is a light-dependent process termed photoactivation (for reviews, see refs *1*, *2*). Photoactivation is a multiquantum process, and the basic kinetic scheme derived from George Cheniae's original studies (*3*−*6*) is widely accepted, although the molecular basis of this process remains to elucidated. Early kinetic analysis suggested that photoactivation involves the formation of two unstable intermediates separated by a light-independent (dark) rearrangement step, which has been estimated to occur with a ∼150 ms half-time. This kinetic model has been termed the "two-quantum series model" (*6*), and its derivatives (*7*−*14*) have not deviated fundamentally from the original formulation (Figure 1A). Note, the formation of "**D**" corresponds to a stable state that readily converts to an O_2-evolving center.

One of the key experiments for demonstrating this kinetic model was Cheniae's paired-flash experiment (*5*), shown schematically in Figure 1B. In this experiment, cyanobacterial cells were extracted with hydroxylamine to remove the active site Mn and then subjected to a xenon light flash protocol consisting of 75 single flashes or pairs of flashes (Δt_1 = 150 ms) separated by longer and variable time intervals (Δt_1 = 0.3 to 8 s). When the variable intervals were long (5 to 8 s), the yield of photoactivated, O_2-evolving centers was only significant if pairs of flashes were given.

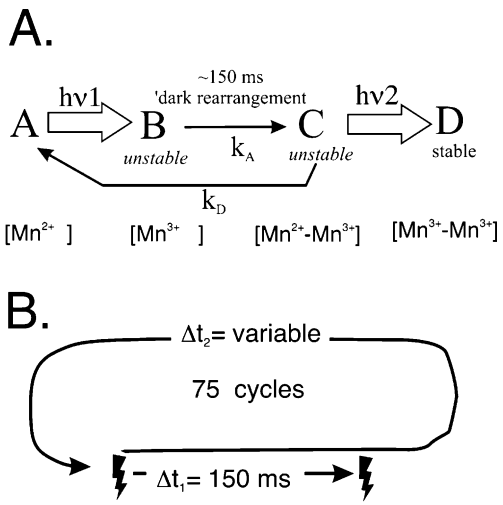

FIGURE 1: (A) The "two-quantum" model of photoactivation. Postulated state of Mn bound to the assembling WOC is shown below. (B) The flash parameters describing the paired-flash photoactivation protocol, modeled after Cheniae (*5*), used for photoactivation of hydroxylamine-extracted *Synechocystis* sp. PCC6803 cells.

† This work was funded by the National Science Foundation (MCB-0448567 to R.L.B.).

* Corresponding author. Phone: 405-744-7445. Fax: 405-744-6790. E-mail: burnap@biochem.okstate.edu.

[1] Abbreviations: DCBQ, 2,6-dichlorobenzoquinone; EDTA, (ethylenedinitrilo)tetraacetic acid; HA, hydroxylamine (NH_2OH); Hepes, 4-(2-hydroxyethyl)-1-piperazineethanesulfonic acid; HBG-11, normal BG-11 growth medium buffered with Hepes−NaOH pH 8; PSII, photosystem II; WOC, H_2O oxidation complex of PSII.

10.1021/bi050069p CCC: $30.25
Published on Web 06/24/2005

The negligible yields for single flashes given at the longer flash intervals were interpreted as demonstrating that at least two light quanta were required to form a stable intermediate in the formation of an O_2-evolving center. Furthermore, two light quanta were sufficient to form the stable intermediate, since additional flashes (e.g. triples) did not significantly improve the quantum yield of the process. These experiments were complemented by measuring the yield of photoactivation resulting from a discrete number of equally spaced flashes given at different intervals. This experiment produces a "bell-shaped" curve that corresponds to low yields for flashes given at short intervals, a maximum at intermediate intervals, and low yields again, at long intervals. The low yields at short flash intervals reflect the existence of a rate-limiting, molecular process **B** → **C** that needs to go to completion before the second quantum can be productively utilized to advance the assembly process. The low yields at long flash intervals reflect the decay of the first photointermediate, **C**, that is lost if the second quantum does not arrive to form the first stable intermediate, **D**, thereby locking in the progress as the **C** ⇒ **D** conversion. The rates of the rearrangement and the decay have been estimated in several systems to be approximately 150 ms and 1 to 8 s, respectively, based upon a kinetic model derived from the scheme shown in Figure 1A. However, over the course of multiple repetitions of the flash interval experiment we have noticed considerable variability in the shape of the bell curve in the short flash interval region. In the context of subsequent experiments, the initial photoact, **A** ⇒ **B**, likely involves the photooxidation of a single Mn^{2+} ion (*15*) bound as the hydroxide, $Mn-OH^{+}$ (*16*), to the high affinity Mn-binding site containing aspartate 170 of the D1 protein of PSII (*17*). Photooxidation of this species, with the formation of intermediate **B**, leads to the refractory period of the dark rearrangement, during which further productive photooxidation of Mn^{2+} cannot occur. The nature of this refractory period in not clear, although it has been speculated that the rearrangement to **C** involves a protein conformational change necessary for the binding and subsequent photooxidation of the second Mn^{2+} (*2*, *18*−*20*).

The following experiments were designed to more thoroughly investigate the kinetics of the dark rearrangement and the labile intermediates of photoactivation. Specifically, we sought to kinetically isolate the dark rearrangement from the decay processes associated with the intermediates by applying a new multiple flash procedure to improve our ability to characterize the molecular aspects of photoactivation. The results presented here suggest that the original model of photoactivation may need modification to account for the existence of two kinetically distinct processes that occur during the assembly process. Preliminary aspects of this work were presented in the Proceedings of International Congress of Photosynthesis, Montreal 2004.

MATERIALS AND METHODS

Strains and Growth Conditions. The glucose-tolerant strain of *Synechocystis* sp. PCC6803 was routinely maintained in BG-11 medium as described previously (*21*). Experimental cultures were propagated in BG-11 media buffered with 20 mM HEPES−NaOH pH 8.0 (HBG-11) under a PFD (photon flux density) of ~80 μmol m^{-2} s^{-1} at 30 °C. Cultures were bubbled with filter sterilized air enriched with 3% CO_2. Light intensity measurements were made with a LiCor sensor (Lincoln, NE).

HA Extraction of Cells. When cultures were in late-log phase and variable fluorescence ($(F_m - F_0)/F_0$) of the culture was over 0.5, approximately 400 mL of cells was pelleted at 25 °C at 5850*g* (Sorvall, GSA rotor) for 10 min. The cells were gently resuspended with a minimal volume of HBG-11 using a paintbrush, and the volume was expanded to 35 mL with additional HBG-11. The washed cells were centrifuged again at 25 °C at 10400*g* for 5 min. The pelleted cells were resuspended as before in HBG-11 medium, and the suspension was adjusted to a Chl concentration of 100 μg mL^{-1} Chl. Hydroxylamine was added to 1 mM from a freshly prepared 100 mM stock adjusted to pH 7, and the treated suspension was incubated for 12 min in the darkness with rotary agitation at room temperature. In later experiments, the pH of the hydroxylamine was not adjusted since it had no discernible effect on the results of extraction and photoactivation, presumably because it was immediately added to a fairly strongly buffed medium (HBG-11). The incubated cells were washed with ~35 mL of HBG-11 medium and pelleted at 25 °C by centrifugation at 10400*g* for 5 min. This washing step was repeated four more times. Finally, the cells were diluted (100 μg Chl/mL) with HBG-11 medium and maintained in the dark on a rotary shaker throughout the course of the experiment.

Photoactivation of HA-Extracted Cells. HA-extracted cells were photoactivated using an EG&G xenon flash lamp receiving a 4.5 J discharge from a 5 μF capacitor connected to a EG&G PS-302 triggered power supply with a flash duration of 5 μs (full-width, at half-maximal peak intensity). A new set of software routines was developed to allow more complex flash patterns and data acquisition. This was implemented using the LabView programming environment (National Instruments, Austin, TX) and using on-board clocks of the data acquisition card (PCI-MIO-16E, National Instruments). Light from the flash lamp was focused vertically down on an open vessel, silvered on the bottom, containing 400 μL of HA-extracted sample in HBG-11 at a concentration of 100 μg Chl mL^{-1}. This medium contains $MnCl_2$ and $CaCl_2$ at concentrations of 10 μM and 245 μM, respectively, although the actual concentrations inside the cells in the thylakoid are difficult to assess. The sample was magnetically stirred during the photoactivation and assay period. Additions to the photoactivation mixture are indicated in the text and figure captions. Light from the xenon flash was determined to be saturating by experiments using neutral density filters. At the completion of the photoactivation flash treatment, 100 μL aliquots were withdrawn for assay for light-saturated rates of O_2 evolution, which were determined using a Clark-type electrode. Photoactivated samples were resuspended in HN (10 mM Hepes, pH 7.2, 30 mM NaCl) buffer supplemented with an artificial electron acceptor system consisting of 1 mM DCBQ and 1 mM potassium ferricyanide, and oxygen evolution was measured in response to saturating red (>620 nm) illumination at 30 °C. Estimation of the kinetics of the dark rearrangement and the decay of the intermediates was obtained by fitting to the equation $Y_n = [k_A/(k_D - k_A)][D]_0(e^{-k_A t_d} - e^{-k_D t_d})$ of Tamura (*7*). Here, Y_n is the yield of active centers on the *n*th flash, $[D]_0$ is the concentration of centers prior to the photoactivation, and the other parameters have the same meaning as in Figure 1A.

Table 1: Maximal Yields of Photoactivation for *Synechocystis* PCC6803

treatment	O_2 evolution[a]
initial activity[b]	851.2 ± 11.2 (100%)
hydroxylamine-extracted[c]	7.3 ± 2.3 (0.86%)
fully photoactivated[d]	784.7 ± 16.3 (92.2%)

[a] O_2 evolution assays were performed with a Clark-type concentration electrode and contained 1.0 mM DCBQ and 1.0 mM KFeCN. Values are expressed as μmol of O_2·(mg Chl)$^{-1}$·h^{-1}. [b] Initial activity measured oxygen evolution of cell culture before treatment of hydroxylamine. [c] After treatment of 1 mM hydroxylamine with cells at a concentration of 100 μg of Chl mL^{-1}, O_2 evolution of cells. [d] After treatment of hydroxylamine, then photoactivated by 2000 Xe flashes given with a time interval of 0.5 s.

Fluorescence Measurements. Measurements of variable fluorescence yields were performed using a Walz PAM 101 chlorophyll fluorometer equipped with PAM 103 flash attachment (Walz Inc., Germany) essentially as described previously (*22*, *23*). Cells were prepared exactly as for the photoactivation experiments monitored by O_2 evolution as described above.

RESULTS AND DISCUSSION

To prepare for a more detailed kinetic analysis of photoactivation of the experimental model *Synechocystis* sp. PCC6803 in vivo, improvements over the original procedures (*5*, *12*) were made in terms of yield and reproducibility (Table 1). Key factors were straightforward: (1) consistent growth and harvesting of cultures using late log phase cells grown with bubbling CO_2-enriched aeration in buffered medium resulted in very high starting activities; (2) care in resuspension and use of growth medium to wash the hydroxylamine-extracted cells enhanced the extent of recovery. The paired-flash experiment (vide supra and Figure 1B) was performed with *Synechocystis* sp. PCC6803 cells using the procedure developed by Cheniae and Martin (*5*). For this experiment, HA-extracted cells were subjected to a flash protocol consisting of 75 single flashes separated by variable dark intervals or pairs of flashes (Δt_1 = 150 ms) followed by a longer and variable (Δt_2 = 0.3 to 8 s) period as shown in Figure 1B. Even though these cells were capable of efficient, high yield photoactivation under a sequence of 2000 flashes given with a time interval of 0.5 s (see Table 1), the level of recovery was very small when the interval between single flashes exceeded 1 s, consistent with the existence of labile intermediates in the photoactivation process (Table 2). However, even pairs of flashes produced very little yield at longer time intervals (Table 2). This result contrasts with the same experiment performed with *Synechococcus elongatus* (quoted in Table 2) where paired flashes gave moderate levels of recovery even with intervals of 5 and 8 s. This experiment was repeated numerous times and under several different preparation and buffer conditions, but all with essentially the same result. This indicates that the photoactivation intermediates are highly labile in *Synechocystis* despite the high level of photoactivation that can be obtained in the same preparation of cells. By comparison with *S. elongatus*, there appear to be fundamental species-specific differences in the photoactivation process in vivo. One possibility is that the amount of reductant available to deactivate the photoactivation intermediates is greater in *Synechocystis* than *Synechococcus*. The presence of an unidentified PSII reductant has been invoked to explain certain PSII fluorescence characteristics (*24*, *25*) and to explain the spontaneous formation of super-reduced forms of the WOC (*26*, *27*) and the associated loss of O_2-evolution activity and presumptive disassembly of the $(Mn)_4$ when mutants lacking the extrinsic proteins are placed in the dark (*11*, *12*, *28*−*30*). Importantly, this result suggests that the so-called first stable intermediate of photoactivation (*3*, *5*, *7*, *10*−*12*, *31*, *32*), **D** in Figure 1A, is actually quite labile in vivo in *Synechocystis*.

To explore the possibility that the increased dark lability of the photoactivation intermediates is due to a PSII reductant, the effects of an artificial electron acceptor were tested. The photoactivation experiment shown in Figure 2 was conducted using the efficient membrane-permeable electron acceptor 2,6-dichlorobenzoquinone (DCBQ), which intercepts electrons at the Q_B site of PSII. It was tested in conjunction with the secondary electron acceptor potassium ferricyanide (KFeCN), which is not membrane permeable. This widely used electron acceptor system supports the high rates of light-saturated O_2-evolution activity in standard assays (Materials and Methods) and has been found to be an efficient acceptor for the photoactivation of HA-extracted wheat PSII membrane preparations (*10*). For this experiment, HA-extracted cells were subjected to a series of 150 flash pairs (Δt_1 = 300 ms, separated by a 10 s interval, Δt_2 = 10 s; see Figure 6, panel A, for scheme) with various concentrations of DCBQ plus 200 μM KFeCN. As shown in Figure 2, the optimum concentration is approximately 50 μM DCBQ under these conditions, which results in enhancement of the yield of photoactivation nearly 2-fold. The optimum DCBQ concentration is higher than the 20 μM DCBQ optimum observed for the in vitro wheat PSII membrane photoactivation system (*10*). The yield of activity in *Synechocystis* cells was less sensitive, but was consistently higher with the addition of KFeCN as the secondary electron acceptor, yet this dependence was not explored fully. Nevertheless, it can be concluded that DCBQ is an efficient PSII electron acceptor for the photoactivation of HA-extracted *Synechocystis* cells.

Despite the nearly 2-fold enhancement of the yield of photoactivation by the addition of DCBQ for the paired-flash experiment, very little change was observed for the increase in O_2-evolution activity as a function of flash number when flashes were given at a constant interval of 0.5 s as shown in Figure 3. Maximal activity was realized after 2000 flashes with or without DCBQ, and DCBQ actually decreased the final yield slightly. Therefore the enhancement seen in the flash pair, long dark interval experiment shown in Figure 2 is likely due to the stabilizing effect that DCBQ has upon the labile dark intermediate(s) of photoactivation.

To analyze the effects of the DCBQ treatment on the acceptor side of PSII during photoactivation, the millisecond kinetics of flash-induced fluorescence yield were monitored using a PAM fluorometer equipped with a xenon flash lamp (*22*, *33*) (Figure 4). With fully photoactivated, intact PSII, the measurement of fluorescence yield after a saturating flash (in the absence of DCMU) primarily traces the transfer of electrons from Q_A^- to plastoquinone at the Q_B site of PSII (*17*, *22*−*24*, *34*). Our detection system cannot accurately

Table 2: Photoactivation of Hydroxylamine Extracted *Synechocystis* sp. PCC6803 Using Single- versus Paired-Flash Illumination

	Cheniae's results[a]			standard conditions			standard + DCBQ and FeCN		
interval (s)	pair[b]	single[c]	pair/single ratio	pair	single	pair/single ratio	pair	single	pair/single ratio
0.3	135	97	1.4	163.7 ± 4.0	94.7 ± 2.5	1.7	188.0 ± 6.6	143.0 ± 19.1	1.3
1	245	142	1.7	175.7 ± 4.0	69.7 ± 1.5	2.5	224.3 ± 7.4	151.7 ± 16.4	1.5
5	106	21	5.0	40.0 ± 1.7	9.0 ± 1.7	4.4	116.0 ± 3.6	30.3 ± 3.8	3.8
8	90	6	15.0	11.0 ± 3.6	4.7 ± 3.1	2.4	69.7 ± 1.5	19.3 ± 5.5	3.6

[a] Quoted results in Table 1 of Cheniae and Martin (*5*) using another cyanobacterium, *Synechococcus elongatus* (formerly *Anacystis nidulans*, a.k.a. *Synechococcus* sp. PCC7942). Note that artificial electron acceptors were not added during photoactivation in the original experiments by Cheniae and Martin (*5*). [b] Paired flashes were separated by an interval (Δt_1 = 150 ms, Figure 1B) of flashes separated by longer and variable time intervals (Δt_1 = 0.3 to 8 s, Figure 1B). Cells were exposed to 75 repetitive paired flashes (150 total flashes). Values are expressed as μmol of O_2 (mg Chl)$^{-1}$ h^{-1}. [c] Single flashes as in footnote *b*, but only one flash separated variable time intervals (Δt_1 = 0.3 to 8, Figure 1B). Hence, cells were exposed to 75 repetitive single photoactivating flashes.

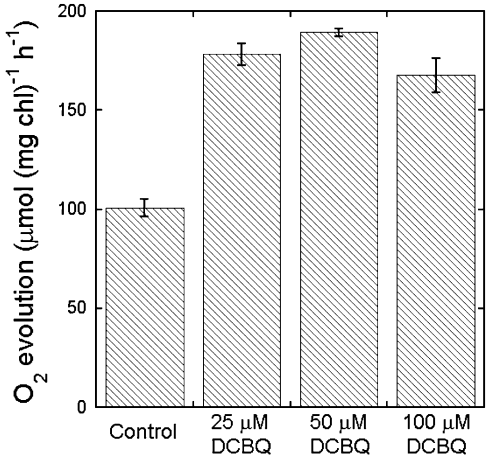

FIGURE 2: Optimizing photoactivation of hydroxylamine-extracted cells with DCBQ plus potassium ferricyanide. HA-extracted cells were subjected to a series of 150 flash pairs (Δt_1 = 300 ms), 300 flashes total, with each flash pair separated by a 10 s interval (Δt_2 = 10 s); in the presence of the indicated concentrations of DCBQ plus a constant amount, 200 μM, of KFeCN, except for the control that had neither DCBQ nor KFeCN added. Error bars indicate standard deviations (n = 3).

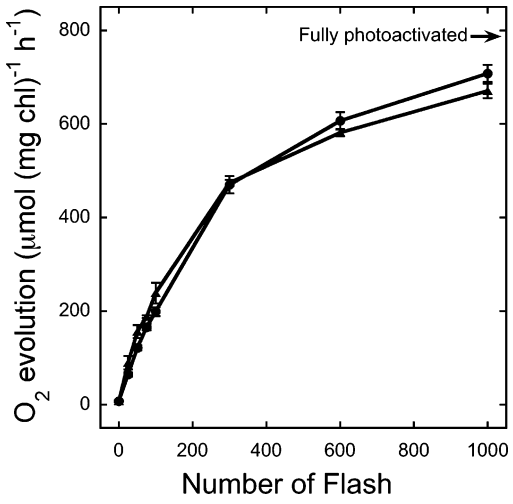

FIGURE 3: Photoactivation of hydroxylamine-extracted cells as a function of the number. Trains of photoactivating varying flashes were given with a uniform interval of 0.5 s to HA-extracted cells in the presence (triangles) or absence (circles) of 50 μM DCBQ plus 200 μM of potassium ferricyanide. Error bars indicate standard deviations (n = 3−5).

measure this fluorescence transient sooner than ~200 μs after the flash, and therefore the early phases of the transient corresponding to the initial rise in fluorescence due to the formation of the highly fluorescent P680-Q_A^- state (nano- to microseconds) and the fast phase of its decay due to the transfer of the electron to the occupant of the Q_B site (~100−200 μs) cannot be observed. However, the millisecond time components of the Q_A^- to Q_B transfer can be observed (*22*, *23*) and provide an indicator of the overall process. In the case of samples undergoing photoactivation, there are additional complications due to the nature of the sample. Most significantly, the rate of electron transfer from Q_A^- to Q_B is dramatically slower in the un-photoactivated state of PSII due to the midpoint redox potential of the Q_A^-/Q_A couple being more positive. The Q_A^-/Q_A couple is +110 mV vs NHE in the absence of the assembled $(Mn)_4$ compared to −80 mV in the fully assembled state (*35*). The increase in the rate of Q_A^- to Q_B transfer during photoactivation is taken as evidence for the coupling of structural changes occurring on the donor and acceptor side of the PSII complex accompanying photoactivation and may have a protective function (*36*, *37*). Ono has used the associated change in fluorescence kinetics as a means of titrating the high affinity Mn^{2+} binding site (*17*) and established that the alteration of the Q_A^- midpoint potential involves the photooxidation of a single Mn^{2+} ion bound to the high affinity site (*15*).

Figure 4A illustrates this conversion of the high potential to low potential form of Q_A^-/Q_A by following the fluorescence transient during the course of photoactivation in HA-extracted *Synechocystis* cells. During the initial stage of photoactivation (after 25 flashes, Figure 4A) there is virtually no decay of fluorescence after the saturating actinic flash. On the other hand, the initial level of fluorescence is relatively high prior to the flash. This is due to the actinic effect of the PAM fluorometer's modulated measuring light combined with the sluggishness of forward Q_A^- to Q_B in the unassembled reaction center. Because of the slow transfer Q_A^- to Q_B, even the relatively weak measuring light results in the accumulation of Q_A^- and hence an accumulation of a large fraction of PSII centers in this high fluorescent state. As an increasing fraction of the PSII centers contain an assembled WOC during the photoactivation process, there is a corresponding increase in the fraction of centers that exhibit the more rapid, Q_A^- to Q_B, transfer kinetics. When this occurs, two things happen in this experimental setup: first, the quasi-equilibrium level of fluorescence immediately prior to the flash begins to approach the true basal level of fluorescence, F_0. Second, the fluorescence transient resulting from the actinic flash forming the P680-Q_A^- state and the subsequent decay of that state due to electron transfer to Q_B

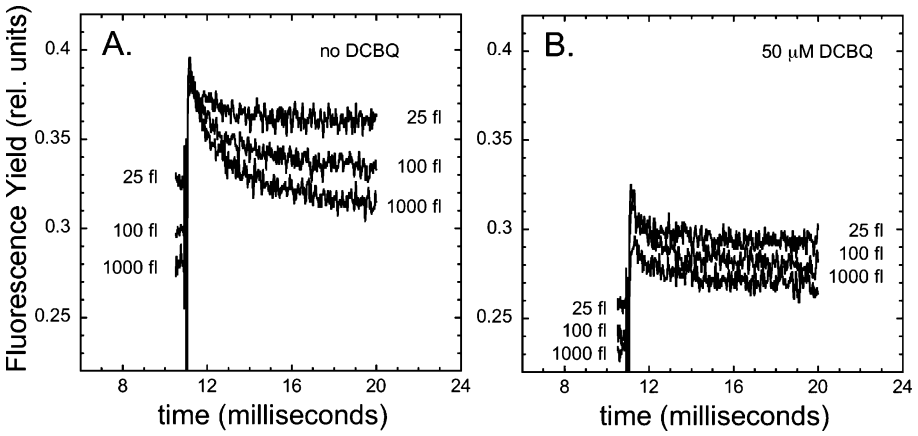

FIGURE 4: DCBQ is an efficient acceptor of electrons and quencher of fluorescence during photoactivation in vivo. Traces were obtained with the same preparation of cells and were treated identically except that panel A is without DCBQ while panel B contains 50 μM DCBQ plus 200 μM potassium ferricyanide. Fluorescence transients were recorded after 25, 100, and 1000 photoactivating flashes as the average of five flash transients after the 20th, 95th, and 995th flashes in the series. The saturating Xe actinic flash (~6 μs fwhm) occurs at 11 ms in this figure and is accompanied by a large negative electronic artifact. The level of fluorescence immediately prior to the flash is equivalent to F_{eq} in ref *23*, except that the quasi-equilibrium concentration of Q_A^- changes as the acceptor side properties change from slow to fast rates of Q_A^- to Q_B transfer in the samples during the photoactivation (see Results and Discussion). The modulated measuring beam automatically is switched from 1.6 to 100 kHz 2 ms before the xenon flash. True F_0 is estimated to be approximately 0.21. Conditions are the same as for the photoactivation experiments in the other figures except that the chlorophyll concentration is 5 μg mL^{-1}.

becomes obvious (note the differences in traces corresponding to increasing numbers of photoactivating flashes, Figure 4A).

The addition of DCBQ to otherwise identical samples (Figure 4B) results in a sharp reduction in fluorescence at all times during the observation of the experiment. Note that the levels of fluorescence in panels A and B are directly comparable since they are derived from identically prepared samples, and high and similar rates of O_2-evolution activity are restored in each by the 1000th photoactivating flash (see Figure 3). The fact that even the preflash quasi-equilibrium level of fluorescence in the plus DCBQ sample (Figure 4B) is lower than in the minus DCBQ control (Figure 4A) suggests that DCBQ is an efficient electron acceptor even in the un-photoactivated state of the acceptor side. This is consistent with the fact that the midpoint potential for DCBQ is approximately +200 mV whereas the estimated midpoint of Q_A^- in the un-photoactivated state is +110 mV (*35*), as mentioned above. It is apparent from these results that DCBQ is also an efficient electron acceptor during photoactivation of *Synechocystis* and suggests that the stabilization of labile photoactivation intermediate(s) by 50 μM DCBQ during protracted intervals of darkness between photoactivating flashes is likely due to the interception of electrons at the acceptor side of PSII. At the same time, caution on this conclusion is warranted owing to the fact that the potential for direct quenching of fluorescence cannot be excluded.

Since Ca^{2+} is an essential component of the WOC and has been shown to be important for the protection of $(Mn)_4$ from reductant in the intact WOC (*38*−*40*) to modulate the kinetics of photoactivation (*13, 14, 18, 41*). Therefore, we tested the effects of added Ca^{2+}, in the presence of the Ca^{2+}-ionophore A23187, on the yields of photoactivation under continuous, equally spaced flashes and in a paired-flash experiment where the decay of intermediates is pronounced (Figure 5). Consistent with its importance in the assembly and function of the WOC, the addition of Ca^{2+} resulted in a modest but significant increase in the yield of photoactivation under continuous flashing at 500 ms intervals. On the other hand, Ca^{2+} did not stabilize the dark labile intermediates in the paired-flash experiment. Since Ca^{2+} is well-established as protecting the assembled $(Mn)_4$ from attack by exogenous reductants (*38*−*40*), the present results may indicate that the rapid destabilization of the photoactivation intermediates in vivo is due to attack by reductant that is internal to the reaction center.

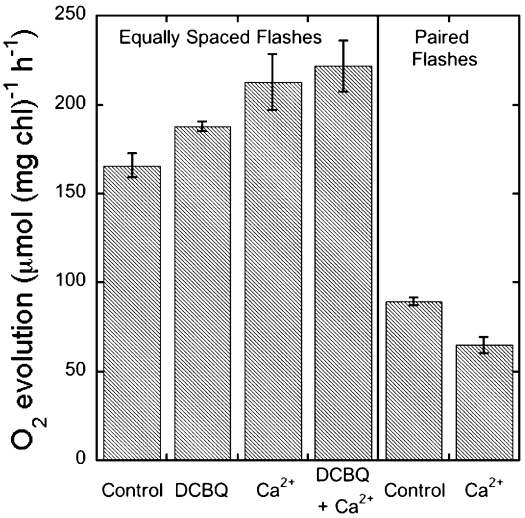

FIGURE 5: Effect of Ca^{2+} on photoactivation of the 75 repetitive paired (right panel) and same space (left panel) flashes of hydroxylamine-extracted cells. Equally spaced flashes with periodicity of 0.5 s. The paired flashes were composed to 150 ms interval between the first and second flashes, and 10 s dark period between the second flash and the first flash of the next cycle. Photoactivation reactions as before but supplemented with the following: (Ca^{2+}) 10 μM A23187, 20 mM $CaCl_2$; (DCBQ) 50 μM DCBQ, 200 μM potassium ferricyanide. Error bars represent standard deviation ($n = 3$).

DCBQ was tested to determine whether it stabilized the intermediates that proved labile during the 10 s dark interval between either single flashes or flash pairs of the Cheniae experiment as summarized in Table 2. Indeed, DCBQ was observed to stabilize the labile dark intermediate(s) of photoactivation under both single and paired-flash illumina-

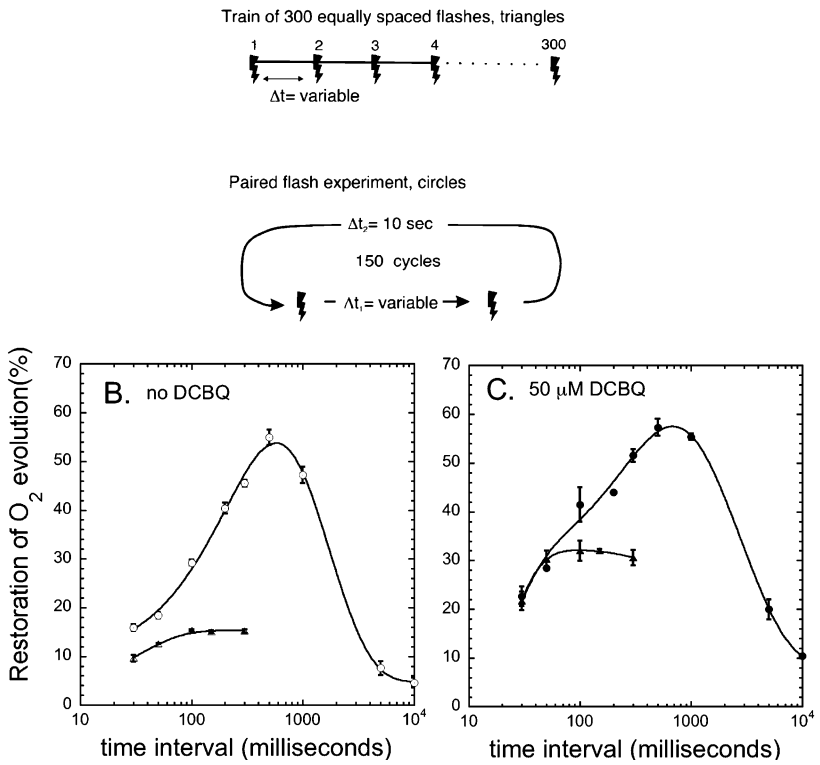

FIGURE 6: Effect of DCBQ on flash interval dependence of photoactivation in hydroxylamine-extracted *Synechocystis* PCC6803 cells. Three hundred flashes were given as pairs separated by a 10 s dark interval (triangles) or as trains of equally spaced flashes (circles) as depicted schematically in panel A. Each data point therefore represents the yield of 300 flashes, with each data point representing the different flash patterns and timings used. HA-extracted cells were photoactivated with (panel B) or without (panel C) 50 μM DCBQ and 200 μM potassium ferricyanide. The data were normalized with respect to the values of fully photoactivated (2000 flashes) replicates. Error bars indicate standard deviations ($n = 3-5$).

tion conditions (Table 2). Considering these results in the context of the two quantum model (Figure 1A): If DCBQ were to specifically stabilize intermediates **B** and/or **C**, rather than **D**, then a greater DCBQ enhancement would be expected for the single-flash protocol than the double flash protocol. However, yields from both protocols are increased by DCBQ (Table 2), and the enhancement (yield with DCBQ ÷ yield without DCBQ) is greater for the paired-flash protocol (69.7 ÷ 11 = 6.3-fold at the 8 s interval) is actually higher than for the single-flash protocol (19.3 ÷ 4.7= 4.1-fold at the 8 s interval). Therefore, DCBQ likely stabilizes several intermediates, including **D**, the "first stable intermediate" (*3*, *5*, *7*, *10*−*12*, *31*, *32*) that is found here to be rather unstable in *Synechocystis*.

Since DCBQ stabilizes labile photoactivation intermediate(s), an estimate of its effects upon the rate of the decay of the intermediates and its effect on the kinetics of the rate-limiting, molecular process **B** → **C**, the "dark rearrangement" step, was examined by further probing the stability of the intermediates under systematically varied dark intervals. Additionally, we sought to better define the kinetics of the process by increasing the number of samples at short time intervals. Figure 6 shows the results of two types of experiment, illustrated schematically in panel A. The first type of experiment involves photoactivation by a finite number of equally spaced flashes, 300 in this case, and repeating this using different flash intervals ranging from a few milliseconds to several seconds (upper scheme, panel A) and measuring the extent of recovery of oxygen evolution for each flash set. Plots of the results of this experiment are shown in panels B (no DCBQ, open circles) and C (50 μM DCBQ, closed circles) of Figure 6 and exhibit a characteristic bell-shaped curve. Addition of DCBQ results in increases in yield at the shorter and longer intervals corresponding to a broadening of the overall curve. The kinetics of the dark rearrangement and decay of intermediates can be estimated from the rising and falling slopes, respectively, of the bell-shaped curve (*3*, *7*, *12*, *20*, *42*−*44*). Accordingly, the overall decay of the intermediates in the dark slowed approximately 2-fold by DCBQ, with estimated half-times of 1 and 2.1 s without and with DCBQ, respectively. This fits with the conclusion that DCBQ stabilizes dark intermediates drawn from the paired-flash experiments (Table 2 and Figure 2). DCBQ was also observed to affect the rising portion of the curve, and, correspondingly, the dark rearrangement has an estimated half-time of 190 and 130 ms without and with DCBQ, respectively. However, the shape of the plus DCBQ curve has a shoulder in the domain of short flash intervals, perhaps suggesting the existence of another kinetic phase observable in DCBQ-treated samples, and therefore these numerical estimates may be misleading since they assume a simple exponential component (*7*, *45*).

The second type of experiment is shown schematically in the lower part of Figure 6, panel A, and is indicated by the open and closed triangular symbols of the adjacent plots in panels B and C. This is a variant of the paired-flash

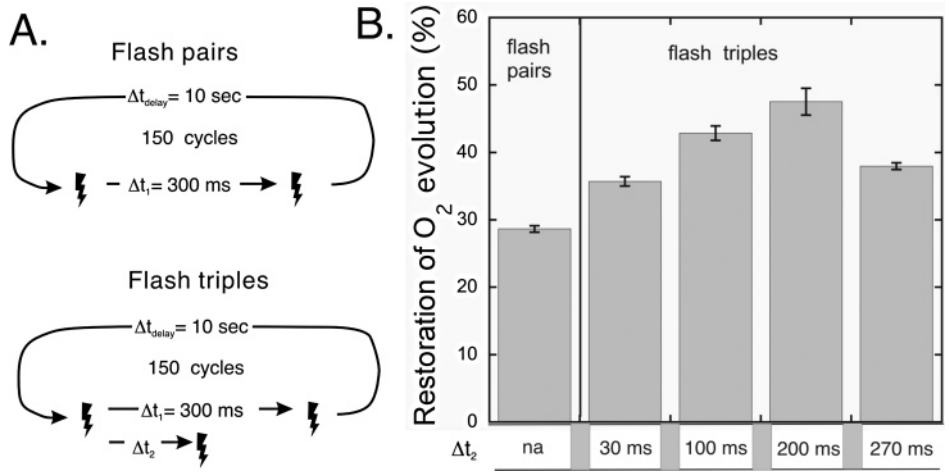

FIGURE 7: Effect of multiple flashes on the yield of photoactivation in hydroxylamine-extracted *Synechocystis* PCC6803 cells. Yields of photoactivation, shown in panel B, due to 300 flashes were given as pairs (left side of panel B) or 450 flashes given as triples (right side of panel B), separated by a 10 s dark interval according to the schemes depicted in panel A. The paired-flash experiment shown in the left portion of panel B yield indicates the restoration of O_2 evolution by 300 pairs of flashes and is similar in design and result to the 50 μM DCBQ, 200 μM potassium ferricyanide treatment of Figure 2. The triple flash experiments, shown in the right portion of panel B, involve an additional flash given at different times relative to the pair of flashes, as indicated in the table below panel B. Each data point therefore represents the yield of 450 flashes, with each column representing the different flash patterns used. All photoactivation reactions were conducted as before in reactions supplemented with 50 μM DCBQ, 200 μM potassium ferricyanide. Error bars represent standard deviation ($n = 3$).

experiment, discussed earlier (Table 2), and involves a constant and relatively long dark period separating pairs of flashes given at short and systematically varied intervals. The idea here is that the long dark interval between paired flashes should allow decay of the dark intermediates **B** and **C** to largely reach completion, according to the two-quantum model, and the spacing of the pairs of flashes should assay for the rate of the dark rearrangement. As with the first type of experiment (equal spacing of flashes, circle symbols), each data point represents the yield of photoactivation after 300 flashes, but with differences due to the timing of the 300 flashes. Without the addition of DCBQ (Figure 6, panel B, open triangles), the yield of photoactivation was small even at intervals that should allow completion of the dark rearrangement, yet still relatively short compared to the 1 s decay time estimated from the bell curve above. This indicates that stability of one or both of the two photointermediates **B** and/or **D** is very low. This, combined with the fact that yields are relatively high with a constant flash interval of 500 ms in the bell curve, indicates a requirement for additional flashes, perhaps to advance the assembly past the binuclear complex (intermediate **D**), before a stable cluster of Mn atoms is formed or to allow the accumulation of a secondary oxidant capable of stabilizing the intermediates.

The addition of DCBQ (Figure 6, panel C, closed triangles) produced an approximately 2-fold increase even at the shortest interval (30 ms) in the paired-flash experiment. At very short flash intervals, the photoactivation yields depend mostly on the efficiency of very rapid processes (quantum yield of the two photoreactions), rather than the slower processes such as the dark rearrangement. Therefore, the efficient electron acceptor activity of DCBQ during photoactivation, as shown in the fluorescence experiment (Figure 4), appears to prevent the loss of intermediates by preventing the back-reaction between Q_A^- and the oxidized Mn produced by the primary photoreactions. Similar conclusions were reached after the efficacy of artificial electron acceptors in the in vitro photoactivation of spinach PSII membranes was analyzed (*10*).

While the increase in yields by DCBQ in the paired-flash experiment is expected given the other results with this electron acceptor, what is remarkable about the paired-flash experiments shown in Figure 6 is what is *not* observed: the rate-limiting dark rearrangement step characterized by the ~150 ms kinetics is absent despite significant yields of oxygen evolving activity. The dependence of the yield increase on flash interval in this paired-flash experiment indicates a process with a half-time of approximately 16 and 23 ms, with and without DCBQ, respectively. These rates are 5- to 10-fold faster than the dark rearrangement time and approach the turnover time overall catalytic cycle of the intact PSII reaction center. Since it seems unlikely that any of the photoactivation intermediates would survive longer than the 10 s dark interval of the paired-flash experiment, the rapid kinetics may indicate one of at least two possibilities in the context of the two-quantum mechanism: (1) a fraction of centers are already configured in the rearranged state **C** during or shortly after the first photoact (**A** ⇒ **B**) of the two-quantum mechanism and thus do not need to reconfigure to state **C** in order to productively utilize the second quantum. For example, if the dark rearrangement (**B** → **C**) is a protein conformational change that does not absolutely depend upon the occurrence of the first photoact (**A** ⇒ **B**), then a fraction of centers may already exist in the "**C**" conformation during the first photoact and the second quantum may thus be productively utilized at a rate determined only by the rate of turnover of the photochemical reaction center. Alternatively, a secondary oxidant is utilized to allow oxidation of intermediate **C** generated from a pair of flashes in a *preceding* cycle (Figure 6A) that succeeds in the **A** → **B** conversion, initiating the rearrangement to **C**, but fails to generate **D** with the second member of the flash pair. To explain the results, the putative oxidant must have a longer lifetime than the 10 s of the dark period, and be able to oxidize bound Mn^{2+} in the **C** state. While this latter

alternative involving the action of a stored oxidant could explain the rapid phase, it still does not readily account for the absence of the 150 ms phase that is anticipated according to the standard formulation of the two-quantum mechanism.

To further probe the kinetics in the experimental format of the paired-flash experiment, a triple flash protocol was devised to determine the effect of an additional flash inserted within the flash pair. This additional flash was given at various times shortly after the first member of the flash pair, but before the second member of the flash pair (see scheme in bottom part of Figure 7, panel A). The enhancement of yield by the insertion of this additional flash was found to be low when placed 30 ms after the first flash, higher 100 ms afterward, and greatest at 200 ms after the first flash (Figure 7B). The enhancement declined as it approached to within 30 ms of the last flash of the set (270 ms after the first flash of the triple, Figure 7B). Analysis of this dependence indicates that the rising portion of this enhancement corresponds to a process with a half-time of approximately 150 ms, presumably the dark rearrangement. The fact that the enhancement declines again as the inserted flash approaches coincidence with the last flash of the triple underlines the importance of the third flash in producing the enhancement. If the inserted flash is to be effective, then it must be given with ample time for a rearrangement after the first of the triple and ample time before the last of the triple. It appears that the inserted flash potentiates the effect of the third flash and that this potentiation requires a recovery time between the first and second and between the second and third flashes of the flash triple. Given the timing, the results suggest that after one flash that follows a long (10 s) dark period, assembling reaction centers are converted to a state that requires the 150 ms rearrangement period for the productivity of the subsequent photoactivating flashes.

CONCLUSIONS

The present experiments demonstrate that the cellular environment of photoactivation has a strong influence on the stability of the photooxidized Mn intermediates formed during the assembly the WOC. The intermediates are considerably more unstable than previously reported. A large component of this instability appears to be the back-reaction of electrons on the acceptor side of the reaction center (e.g. Q_A^-) with the oxidized intermediates leading to the formation of the $(Mn)_4$ cluster, as illustrated by the stabilizing effects of the electron acceptor, DCBQ. While DCBQ generally enhanced the yields of photoactivation under most conditions, the most pronounced effect was found in the paired-flash experiments (e.g. Figure 6, compare triangular symbols). Besides the unexpected degree of instability of intermediates, an assembly phase that is 10-fold faster than the previously identified rate-limiting dark rearrangement was observed.

ACKNOWLEDGMENT

We wish to thank Prof. Noriaki Tamura for his useful advice and insight.

REFERENCES

1. Ono, T. (2001) Metallo-radical hypothesis for photoassembly of $(Mn)_4$-cluster of photosynthetic oxygen evolving complex, *Biochim. Biophys. Acta 1503*, 40−51.
2. Burnap, R. L. (2004) D1 protein processing and Mn cluster assembly in light of the emerging photosystem II structure, *Phys. Chem. Chem. Phys. 6*, 4803−4809.
3. Cheniae, G. M., and Martin, I. F. (1971) Photoactivation of the manganese catalyst of O_2 evolution. I. Biochemical and kinetic aspects, *Biochim. Biophys. Acta 253*, 167−181.
4. Cheniae, G. M., and Martin, I. F. (1971) Effects of hydroxylamine on photosystem II. I. Factors affecting the decay of O_2 evolution, *Plant Physiol. 47*, 568−575.
5. Cheniae, G. M., and Martin, I. F. (1972) Effects of hydroxylamine on photosystem II. II Photoreversal of the NH_2OH destruction of O_2 evolution, *Plant Physiol. 50*, 87−94.
6. Radmer, R., and Cheniae, G. M. (1971) Photoactivation of the manganese catalyst of O_2 evolution. II. A two quantum mechanism, *Biochim. Biophys. Acta 253*, 182−186.
7. Tamura, N., and Cheniae, G. (1987) Photoactivation of the water-oxidizing complex in photosystem II membranes depleted of Mn and extrinsic proteins. I. Biochemical and kinetic characterization, *Biochim. Biophys. Acta 890*, 179−194.
8. Miller, A.-F., and Brudvig, G. W. (1989) Manganese and calcium requirements for reconstitution of oxygen evolution activity in manganese-depleted photosystem II membranes, *Biochemistry 28*, 8181−8190.
9. Miyao, M., and Inoue, Y. (1991) An improved procedure for the photoactivation of photosynthetic oxygen evolution: Effect of artificial electron acceptors on the photoactivation yield of NH_2-OH-treated wheat photosystem II membranes, *Biochim. Biophys. Acta 1056*, 47−56.
10. Miyao Tokutomi, M., and Inoue, Y. (1992) Improvement by benzoquinones of the quantum yield of photoactivation of photosynthetic oxygen evolution: direct evidence for the two quantum mechanism, *Biochemistry 31*, 526−532.
11. Burnap, R. L., Qian, M., Al-Khaldi, S., and Pierce, C. (1995) Photoactivation and S-state cycling kinetics in photosystem II mutants in *Synechocystis* sp. PCC6803, in *Photosynthesis: from light to biosphere* (Mathis, P., Ed.) Kluwer Academic Publishers, Dordrecht, The Netherlands.
12. Burnap, R. L., Qian, M., and Pierce, C. (1996) The manganese-stabilizing protein (MSP) of photosystem II modifies the *in vivo* deactivation and photoactivation kinetics of the H_2O-oxidation complex in *Synechocystis* sp. PCC6803, *Biochemistry 35*, 874−882.
13. Ananyev, G. M., and Dismukes, G. C. (1996) High resolution kinetic studies of the reassembly of the tetra manganese cluster of photosynthetic water oxidation: proton equilibrium, cations, and electrostatics, *Biochemistry 35*, 14608−14617.
14. Zaltsman, L., Ananyev, G. M., Bruntrager, E., and Dismukes, G. C. (1997) Quantitative kinetic model for photoassembly of the photosynthetic water oxidase from its inorganic constituents: requirements for manganese and calcium in the kinetically resolved steps, *Biochemistry 36*, 8914−8922.
15. Ono, T. A., and Mino, H. (1999) Unique binding site for Mn^{2+} ion responsible for reducing an oxidized Y_Z tyrosine in manganese-depleted photosystem II membranes, *Biochemistry 38*, 8778−8785.
16. Ananyev, G. M., Murphy, A., Abe, Y., and Dismukes, G. C. (1999) Remarkable affinity and selectivity for Cs^+ and uranyl (UO_2^{2+}) binding to the manganese site of the apo-water oxidation complex of photosystem II, *Biochemistry 38*, 7200−7209.
17. Nixon, P. J., and Diner, B. A. (1992) Aspartate 170 of the photosystem II reaction center polypeptide D1 is involved in the assembly of the oxygen evolving manganese cluster, *Biochemistry 31*, 942−948.
18. Chen, C., Kazimir, J., and Cheniae, G. M. (1995) Calcium modulates the photoassembly of photosystem II $(Mn)_4$ clusters by preventing ligation of nonfunctional high valency states of manganese, *Biochemistry 34*, 13511−13526.
19. Ananyev, G. M., and Dismukes, G. C. (1996) Assembly of the tetra Mn site of photosynthetic water oxidation by photoactivation: Mn stoichiometry and detection of a new intermediate, *Biochemistry 35*, 4102−4109.
20. Qian, M., Dao, L., Debus, R. J., and Burnap, R. L. (1999) Impact of mutations within the putative Ca^{2+}-binding lumenal interhelical a-b loop of the photosystem II D1 protein on the kinetics of photoactivation and H_2O-oxidation in Synechocystis sp. PCC6803, *Biochemistry 38*, 6070−6081.
21. Williams, J. G. K. (1988) Construction of specific mutations in Photosystem II photosynthetic reaction center by genetic engineering methods in Synechocystis 6803, *Methods Enzymol. 167*, 766−778.

22. Li, Z., Bricker, T. M., and Burnap, R. (2000) Kinetic characterization of His-tagged CP47 photosystem II in Synechocystis sp. PCC6803, *Biochim. Biophys. Acta 1460*, 384−389.
23. Chu, H.-A., Nguyen, A. P., and Debus, R. A. (1994) Site-directed mutagenesis of photosynthetic oxygen evolution: Instability or inefficient assembly of the manganese cluster *in vivo*, *Biochemistry 33*, 6137−6149.
24. Philbrick, J. B., Diner, B. A., and Zilinskas, B. A. (1991) Construction and characterization of cyanobacterial mutants lacking the manganese-stabilizing polypeptide of Photosystem II, *J. Biol. Chem. 266*, 13370−13376.
25. Chu, H.-A., Nguyen, A. P., and Debus, R. A. (1994) Site-directed mutagenesis of photosynthetic oxygen evolution: Increased binding or photooxidation of manganese in the absence of the extrinsic 33-kDa polypeptide *in vivo*, *Biochemistry 33*, 6150−6157.
26. Meunier, P. C., Burnap, R. L., and Sherman, L. A. (1995) Modelling of the S-state mechanism and Photosystem II manganese photoactivation in cyanobacteria, *Photosynth. Res. 47*, 61−76.
27. Meunier, P. C., Burnap, R. L., and Sherman, L. A. (1995) Interactions of the photosynthetic and respiratory electron transport chains producing slow apparent O_2 releases under flashing light in Synechocystis sp. PCC 6803, *Photosynth. Res. 45*, 31−40.
28. Gleiter, H. M., Haag, E., Shen, J. R., Eaton Rye, J. J., Seeliger, A. G., Inoue, Y., Vermaas, W. F., and Renger, G. (1995) Involvement of the CP47 protein in stabilization and photoactivation of a functional water oxidizing complex in the cyanobacterium Synechocystis sp. PCC 6803, *Biochemistry 34*, 6847−6856.
29. Engels, D. H., Lott, A., Schmid, G. H., and Pistorious, E. K. (1994) Inactivation of the water-oxidizing enzyme in manganese stabilizing protein-free cells of the cyanobacteria Synechococcus PCC7942 and Synechocystis PCC6803 during dark incubation and conditions leading to photoactivation, *Photosynth. Res. 42*, 227−244.
30. Shen, J. R., Burnap, R. L., and Inoue, Y. (1995) An independent role of cytochrome c 550 in cyanobacterial photosystem, *Biochemistry 34*, 12661−12668.
31. Tamura, N., Kuwahara, M., Sasaki, Y., Wakamatsu, K., and Oku, T. (1997) Redox dependence for photoligation of manganese to the apo water oxidizing complex in chloroplasts and photosystem II membranes, *Biochemistry 36*, 6171−6177.
32. Miyao, M., and Murata, N. (1985) The Cl^- effect on photosynthetic oxygen evolution: interaction of Cl^- with 18-kDa, 24-kDa and 33-kDa proteins, *FEBS Lett. 180*, 303−308.
33. Boerner, R. J., Nguyen, A. P., Barry, B. A., and Debus, R. J. (1992) Evidence from directed mutagenesis that aspartate 170 of the D1 polypeptide influences the assembly and-or stability of the manganese cluster in the photosynthetic water-splitting complex, *Biochemistry 31*, 6660−6672.
34. Nixon, P. J., Trost, J. T., and Diner, B. A. (1992) Role of the carboxy terminus of polypeptide D1 in the assembly of a functional water oxidizing manganese cluster in photosystem II of the cyanobacterium Synechocystis sp. PCC 6803: assembly requires a free carboxyl group at C terminal position 344, *Biochemistry 31*, 10859−10871.
35. Johnson, G. N., Rutherford, A. W., and Krieger, A. (1995) A change in the midpoint potential of the quinone Q_A in photosystem II associated with photoactivation of oxygen evolution, *Biochim. Biophys. Acta 1229*, 202−207.
36. Magnuson, A., Rova, M., Mamedov, F., Fredriksson, P. O., and Styring, S. (1999) The role of cytochrome b559 and tyrosineD in protection against photoinhibition during in vivo photoactivation of photosystem II, *Biochim. Biophys. Acta 1411*, 180−191.
37. Rova, M., Mamedov, F., Magnuson, A., Fredriksson, P. O., and Styring, S. (1998) Coupled activation of the donor and the acceptor side of photosystem II during photoactivation of the oxygen evolving cluster, *Biochemistry 37*, 11039−11045.
38. Sivaraja, M., Tso, J., and Dismukes, G. C. (1989) A calcium-specific site influences the structure and activity of the manganese cluster responsible for photosynthetic water oxidation, *Biochemistry 28*, 9459−9464.
39. Mei, R., and Yocum, C. F. (1991) Calcium retards NH_2OH inhibition of O_2 evolution activity by stabilization of Mn^{2+} binding to Photosystem II, *Biochemistry 30*, 7863−7842.
40. Mei, R., and Yocum, C. F. (1992) Comparative properties of hydroquinone and hydroxylamine reduction of the Ca^{2+}stablilized O_2-evolving complex of photosystem II: Reductant-dependent Mn^{2+} formation and activity inhibition, *Biochemistry 31*, 8449−8454.
41. Ono, T. A., and Inoue, Y. (1983) Requirement of divalent cations for photoactivation of the latent water oxidation system in intact chloroplasts from flashed leaves, *Biochim. Biophys. Acta 723*, 191−201.
42. Debus, R. J., Campbell, K. A., Gregor, W., Li, Z. L., Burnap, R. L., and Britt, R. D. (2001) Does histidine 332 of the D1 polypeptide ligate the manganese cluster in photosystem II? An electron spin echo envelope modulation study, *Biochemistry 40*, 3690−3699.
43. Qian, M., Al Khaldi, S. F., Putnam Evans, C., Bricker, T. M., and Burnap, R. L. (1997) Photoassembly of the photosystem II (Mn)4 cluster in site directed mutants impaired in the binding of the manganese stabilizing protein, *Biochemistry 36*, 15244−15252.
44. Li, Z. L., and Burnap, R. L. (2001) Mutations of arginine 64 within the putative Ca(2+)-binding lumenal interhelical a-b loop of the photosystem II D1 protein disrupt binding of the manganese stabilizing protein and cytochrome c(550) in Synechocystis sp. PCC6803, *Biochemistry 40*, 10350−10359.
45. Ishikawa, Y., Yamamoto, Y., Otsubo, M., Theg, S. M., and Tamura, N. (2002) Chemical modification of amine groups on PS II protein(s) retards photoassembly of the photosynthetic water-oxidizing complex, *Biochemistry 41*, 1972−1980.

BI050069P